Journal of Chromatography, 99 (1974) 407–424

CHROM. 7616

CONSIDERATIONS OF SMALL PARTICLES IN DIFFERENT MODES OF LIQUID CHROMATOGRAPHY

RICHARD V. VIVILECCHIA, RICHARD L. COTTER, ROBERT J. LIMPERT, NORMA Z. THIMOT and JAMES N. LITTLE

Waters Associates Inc., Maple Street, Milford, Mass. 01757 (U.S.A.)

SUMMARY

The use of column packings with particle sizes of 10 μ in different modes of column chromatography, liquid–solid (LSC), bonded phase (BPC) and gel permeation (GPC), was investigated. LSC columns of very high efficiency, 10 effective plates/sec, and high reproducibility were produced by packing μPorasil®, a silica gel with a surface area of 400 m^2/g and an average particle size of 10 μ, into drilled stainless-steel tubes. Bonded phases were prepared by the reaction of monomeric organosilanes with μPorasil to form monomolecular bonded layers. Octadecyl, aminopropyl and cyanopropyl groups were bound to the surface. Packed columns of the monomolecular, bonded phases gave very high efficiencies. More than 3000 theoretical plates and 10 effective plates/sec can easily be obtained on a single 30-cm-long column at a carrier velocity of 0.7 cm/sec. High-speed GPC was performed by using packed columns of μStyragel®, a porous polymer of styrene and divinylbenzene, with average particle sizes of 20 μ. Columns packed with μStyragel (d_p = 10 μ) gave 4000–10,000 theoretical plates/30 cm of column, depending upon the carrier velocity. Molecular-weight distributions of many polymers can be obtained in 10–15 min. In addition, the columns were also run at lower carrier velocities to separate small molecules which differ by as little as one methylene group.

INTRODUCTION

A number of independent investigators[1–8] have experimentally confirmed the theoretical prediction that increased column efficiency in all modes of liquid chromatography (LC) can be obtained by reducing support particle diameter (d_p). Until recently, particles of $d_p < 30\,\mu$ have proved difficult to pack reproducibly. Huber[9] successfully packed kieselguhr of d_p = 5–15 μ by a dry packing technique. The more common technique used to pack particles with $d_p < 20\,\mu$ is the balanced density method[3,4,6], where the density of the dispersing agent is adjusted to that of the particles. Recently, Asshauer and Halász[4] have studied the reproducibility and efficiency of columns packed with 10 μ silica. Using a balance density technique, their results indicate that better reproducibility and peak symmetry are obtained if the inside

diameters of the column tubes are drilled. In addition, excellent columns were also produced with dispersing agents of high viscosity (40–60 cP).

The very high column efficiencies resulting from the use of porous particles of $d_p < 10\,\mu$ are due to the shorter distances the solute molecules must diffuse within the packed bed. The solute molecules undergo more rapid mass transfer between the mobile-phase flow currents or in the stationary phase and/or in the stagnant mobile phase within the pores of the particle[5]. These advantages are gained in all modes of LC: liquid–solid (LSC), liquid–liquid (LLC), bonded phase (BPC), or gel permeation (GPC). This paper will describe the use of small-particle ($d_p < 10\,\mu$) supports in LSC, BPC and GPC.

EXPERIMENTAL

Apparatus

The Waters Associates Model ALC/GPC 202/401 liquid chromatograph (Waters Ass., Milford, Mass., U.S.A.) was used throughout this work. The system employs the Waters M6000 pumping system, capable of delivering flows to 9.9 ml/min up to 6000 p.s.i. Injections were made with the Waters Model U6K universal injector, a septumless high-pressure (6000 p.s.i.) valve injector capable of delivering variable sample sizes from a fraction of 1 μl to 2 ml without changing loop volumes. A 25-μl syringe (Precision Sampling, Baton Rouge, La., U.S.A.) was used to load the valve. Detection was made by a UV monitor at 254 nm or by the Waters Model R401 refractive index detector coupled in series.

The packed columns of silica or bonded phases were constructed of 30 cm × 6.35 mm O.D. seamless, 316 stainless tubing. To achieve highly reproducible, high-efficiency packed columns, the internal surfaces of the tubes were modified to remove the surface porosity and longitudinal striations by a drilling process* first described by Asshauer and Halász[4]. The internal diameter was about 4 mm. The μStyragel® columns were constructed of 30 cm × 9.52 mm O.D. (7.6 mm I.D.) seamless, 316 stainless-steel tubing. The column end-fittings were reducing unions (Parker Hannifin, Oakland, Calif., U.S.A.) modified for minimum dead volume. A stainless-steel frit of 2-μ average porosity (Mott Metalurgical, Farmington, Conn., U.S.A.) was pressed into the end-fitting to contain the packing. In addition, a disc of hardened quantitative filter paper was placed between the frit and the column packing in the case of the bonded phases and silica columns.

Chemicals

The chromatographic solvents were distilled-in-glass from Burdick and Jackson Labs. (Muskegon, Mich., U.S.A.). The tetrabromoethane was purified by passage through a column packed with Woelm basic alumina (ICN Pharmaceuticals, Cleveland, Ohio, U.S.A.).

Packings

The adsorbent was μPorasil® (Waters Ass.), a silica gel of about 400 m²/g surface area, an average pore size of 100 Å and a particle size distribution of 8–12 μ.

* Patent pending.

The adsorbent was packed into drilled 4-mm-I.D. tubes by a balance density technique[4].

The bonded phases were prepared by reacting an organo functional silane with μPorasil®. The silanes used in this work were octadecyltrichlorosilane (Dow Corning, Midland, Mich., U.S.A.), γ-aminopropyltriethoxysilane (Union Carbide, New York, N.Y., U.S.A.), and γ-cyanopropylmethyldichlorosilane (Silar Lab., Watervliet, N.Y., U.S.A.). Reactions were performed under anhydrous conditions to prevent silane polymerization. These packings will be referred to as μBondapak® C_{18}, CN or NH_2. These materials were packed into 30 cm × 4 mm I.D. drilled tubes by a high-viscosity slurry technique[4].

The μStyragel® (Waters Ass.), porous spherical polymer beads of styrene and divinylbenzene for GPC, was prepared in various pore sizes with $d_p < 30\,\mu$. Narrow particle-size distributions were produced by air classification. Fractions with $d_p > 30\,\mu$ were prepared by dry sieving. Slurries of the Styragel® in methanol–chloroform mixtures were packed into columns of 30-cm length. The sample used to calculate the plate height, h, and linear velocity, u, was 6% solution of toluene in tetrahydrofuran (THF). The carrier solvent was THF. The h *vs.* u curves were determined with two packed columns in series.

The particle size distributions of all the supports were determined by a Coulter Counter® Model T_A particle size analyzer (Coulter Electronics, Hialeah, Fla., U.S.A.).

RESULTS AND DISCUSSION

Liquid–solid chromatography

Fig. 1 shows a rapid and efficient separation of a synthetic sample using a column packed with μPorasil®, a silica gel with a particle size distribution of 8–12 μ

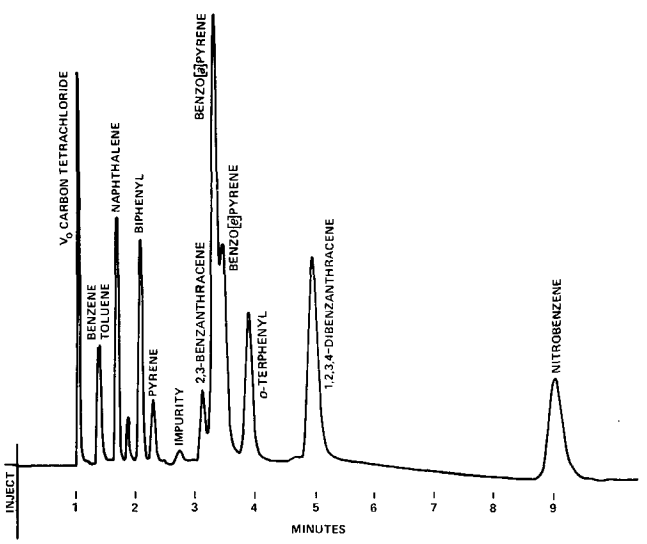

Fig. 1. Separation of a synthetic sample of aromatic compounds with μPorasil columns. Column dimensions, 2 × 300 mm × 4 mm I.D.; d_p 8–12 μ; mobile phase, hexane; flow-rate, 8.0 ml/min; temperature, ambient.

TABLE I

CHROMATOGRAPHIC DATA FOR PACKED COLUMNS OF μPORASIL AND BONDED PHASE CHROMATOGRAPHIC PACKINGS

Column, 30 cm × 4 mm I.D.; mobile-phase velocity, 7.0 mm/sec.

Mobile phase	*Packing*	*Solute*	k'	h	n	$n_{eff.}$	$n_{eff.}$/sec
Hexane	μPorasil	Carbon tetrachloride	0	0.09	3333	0	0
		Benzene	0.3	0.07	4286	228	4
		o-Terphenyl	2.8	0.09	3333	1810	11
		Nitrobenzene	8.1	0.06	5000	3961	10
Hexane	μBondapak NH_2	Carbon tetrachloride	0	0.10	3000	0	0
		p-Chloronitrobenzene	1.1	0.07	4286	1176	12
		m-Chloronitrobenzene	1.5	0.08	3750	1350	13
		o-Chloronitrobenzene	3.2	0.08	3750	2177	12
Hexane–methylene chloride (65:35)		*o*-Nitroaniline	1.0	0.11	2727	682	8
		m-Nitroaniline	1.7	0.08	3750	1487	13
		p-Nitroaniline	4.6	0.09	3333	2249	9
Hexane	μBondapak CN	Carbon tetrachloride	0	0.17	1765	0	0
		m-Chloronitrobenzene	0.5	0.17	1765	196	3
		p-Chloronitrobenzene	0.6	0.15	2000	281	4
		o-Chloronitrobenzene	0.9	0.14	2143	481	6
		m-Dinitrobenzene	2.5	0.15	2000	1020	7
Acetonitrile–water (60:40)	μBondapak C_{18}	Uracil	0	0.08	3750	0	0
		Benzene	1.8	0.08	3750	1550	13
		Acenaphthene	4.6	0.09	3333	2249	9
Acetonitrile–water (40:60)		*p*-Phenylphenol	14.6	0.11	2727	2389	4

and with a surface area of 400 m^2/g. The data in Table I show the high efficiencies of such columns. The h values are nearly independent of the capacity factor k', indicating fast mass transfer within the packed bed. At a mobile phase velocity of 7 mm/sec, nitrobenzene ($k' = 8.1$) showed 10 effective plates/sec. Table II compares the values of $n_{eff.}$/sec obtained by other authors with small-particle silica columns. The values for the μPorasil columns are in agreement with the values observed by other authors.

In order to pack such highly efficient columns reproducibly, a special column finishing process was used as described by Asshauer and Halász[4]. This process involves removing the porous layer and longitudinal grooves from internal walls of seamless, cold-drawn, stainless-steel tubing. Fig. 2 shows the electronmicrographs of the internal surfaces of undrilled stainless-steel tubing, precision bore tubing and drilled

TABLE II

COMPARISON OF SOME PUBLISHED DATA

Column type	k'	$n_{eff.}$/sec	*u (cm/sec)*	*Ref.*
Porous silica microspheres (8–9 μ)	10	14	4.7	2
Silica gel (5–10 μ)	11	10.7	3.2	3
Silica gel (8–12 μ)	6	10	2.0	4
Silica gel (13.2 μ)	1.2	4.3	1.0	1
μPorasil (8–12 μ)	8.1	10	0.7	

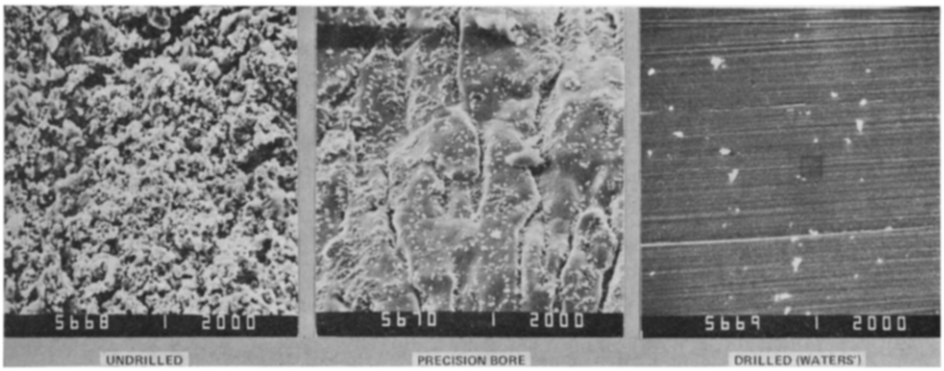

Fig. 2. Electronmicrographs of LC tubing. Comparison of internal surface finishes. Magnification, 2000×.

stainless-steel tubing. The drilling process removes the longitudinal grooves and porous layer which can cause band asymmetry[4].

The variation of the column permeability, K^0, was observed to be very small. An average value of 1.1×10^{-9} cm^2 $\pm 5\%$ was obtained. Assuming that $K^0 \approx d_p^2/1000$, the calculated value of the particle diameter is 10.5 μ, which is in agreement with the experimentally determined particle size distribution.

The separation of complex mixtures or compounds having separation factors close to unity may require more theoretical plates than a single μPorasil column can generate. In such cases, more than one column can be connected in series. Fig. 3 shows the *h vs. u* curves for two individual μPorasil columns (curve A) and the two columns connected in series (curve B) via a 2-in. section of 0.009-in.-I.D. tubing. Less than 10% reduction in plate count from theoretical value was observed. In addition three columns in series were run in the recycle mode to generate even higher plate counts. After 17 passes through 90 cm of μPorasil columns, 46,000 plates were generated for benzo[*e*]pyrene, $k' = 2.4$ (ref. 10). This plate count is sufficient to separate a pair of substances with a separation factor of 1.03 to a resolution of 1.

Bonded phase chromatography

In conventional LLC, a liquid coated on a solid support is in equilibrium with

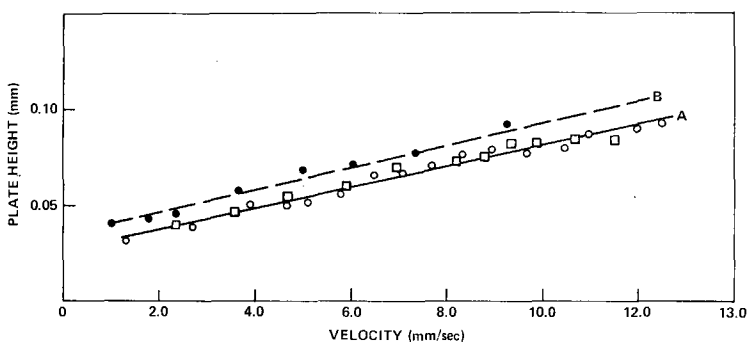

Fig. 3. *h vs. u* curves for two separate μPorasil columns (curve A) and for the two columns connected in series (curve B). Mobile phase: hexane; solute, nitrobenzene, $k' = 8$.

the mobile phase saturated with a stationary liquid. Such a system has a number of disadvantages: (1) the system temperature must be controlled carefully, (2) the stationary phase can be removed by shear forces at high flow-rates, (3) solvent programming is not feasible, and (4) in preparative chromatography, the sample is contaminated with the stationary phase.

To overcome these disadvantages, column packings with chemically bonded, organic, stationary phases have been developed. Three types of bonds can be distinguished in which functional groups are fixed to the surface of a silica support.

(1) *Esterified siliceous supports (brushes).* Esterification of the surface-active silanol groups (Si–O–H) of silica with alcohols creates the Si–O–C bond[11]. These phases have found use in gas and liquid chromatography[12,13]. The disadvantage of esterified supports in LC is the hydrolytic instability of the Si–O–C bond.

(2) *Silicon–carbon bonds.* Si–C bonds are more thermally and hydrolytically stable and consequently are more promising for LC. The stability of the Si–C bond is dependent upon the group attached to the silica atom[14]. The silica atom attached to an unsubstituted aliphatic carbon atom is generally stable in the range $1 < pH < 9$. A number of techniques have been developed for the synthesis of Si–C bonds. Chemically bonded silicone polymers have been prepared by the reaction of organochlorosilanes or organoalkoxysilanes with active surface hydroxyls and subsequent polymerization[15–23]. Another technique involves the synthesis of monomolecular, brush-type phases by the reaction of surface chlorinated silica with Grignard or alkyllithium reagents[24,25].

(3) *Silicon–nitrogen bonds.* Si–N bonds are prepared by the reaction of chlorinated silica with amines or substituted amines[26]. Since a wide variety of amines having varying functional groups are readily available, this technique offers easy access to phases with varying surface polarity. However, the limited pH stability (pH 5–7) is a disadvantage in some forms of chromatography, especially ion-exchange.

The bonded phases prepared in this work involved the reaction of monomeric chloro- or alkoxysilanes with μPorasil to form monomolecular, bonded layers. Monomolecular layers have distinct advantages over polymeric layers, especially with small particles. First, mass transfer in polymeric stationary phases has been shown to be slow[27]. Thus, the performance gains of particle size reduction would be minimal. Secondly, polymeric layers can be expected to shrink or swell with different mobile phases, leading to the probable formation of voids or channels and to varying column permeability.

The surface coverage of the prepared bonded phases is shown in Table III. The surface coverage variation was about 5% from batch to batch. The concentration

TABLE III

SURFACE COVERAGES OF BONDED PHASES

Bonded phase	*Surface coverage (μmoles/m²)*
μBondapak C_{18}	1.0
μBondapak CN	2.8
μBondapak NH_2	3.2

of surface silanol groups has been measured by a number of techniques to be about 8 μmole/m^2 (ref. 28). The extent of reaction of the silanes with silanol groups depends upon the molecular size of the silane. The data in Table III indicate that only a fraction of the silanol groups react, a result that has been observed by a number of workers[28–30]. To reduce the number of accessible silanols, a second-step silanization is performed in the C_{18} and CN synthesis. However, residual silanols still remain after the second-step silanization. Methyl red adsorption tests are negative, indicating that the residual silanols are not readily accessible. Chromatographic experiments using hexane, without water saturation or addition of isopropanol, as the mobile phase did not show marked tailing with test samples. The asymmetry factor, As^2, as defined by Asshauer and Halász[4] varies between 1.5 and 4. Fig. 4 shows the small amount of tailing observed for the separation of nitroanilines on a μBondapak NH_2 column.

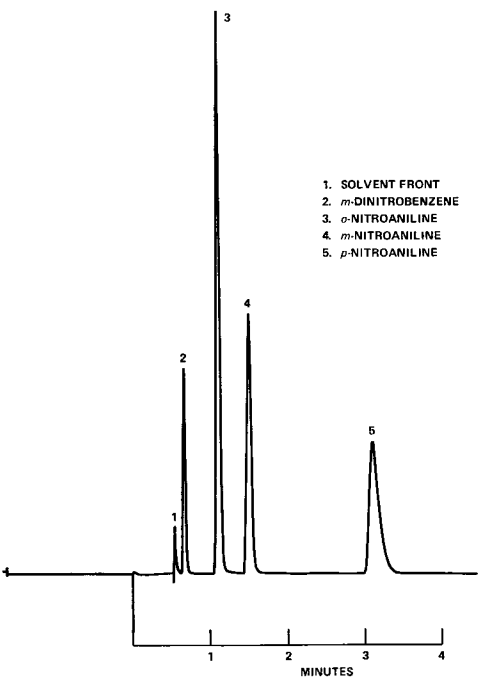

Fig. 4. Separation of nitroanilines. Column: μBondapak NH_2, 300 mm × 4 mm I.D.; mobile phase, hexane–methylene chloride (65:35); flow-rate, 6 ml/min; temperature, ambient.

Fig. 5 illustrates the excellent efficiencies obtained with packed columns of these materials. As a comparison, an *h vs. u* curve of a μPorasil column is included. The *h vs. u* curves were determined in the mobile phase velocity range of 0.8–15 mm/sec. In this range, the simple relationship

$$h = A + Cu$$

is a good approximation[4], where A is the eddy diffusion term and C is the resistance to mass transfer term (the slope of the *h vs. u* curve). Note that the slopes of the μBondapak NH_2 and CN are similar in magnitude to that of the μPorasil column.

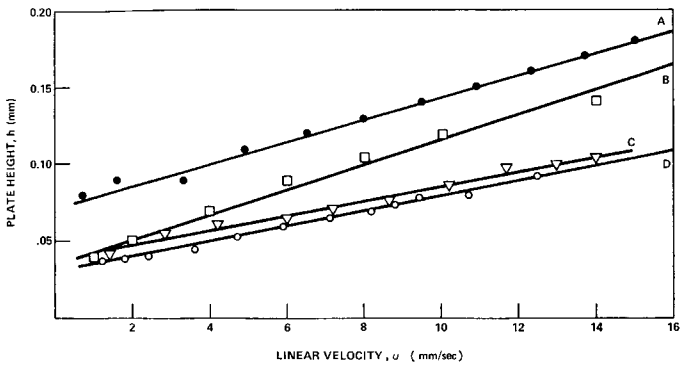

Fig. 5. *h vs. u* curves of packed columns of bonded phases. Column dimensions: 300 mm × 4 mm I.D.; temperature, ambient. (A) μBondapak CN; solute, *o*-chloronitrobenzene, $k' = 0.9$; mobile phase, hexane. (B) μBondapak C_{18}; solute, acenaphthene, $k' = 4.6$; mobile phase, acetonitrile–water (60:40). (C) μBondapak NH_2; solute, *m*-chloronitrobenzene, $k' = 1.5$; mobile phase, hexane. (D) μPorasil; solute, nitrobenzene, $k' = 8.1$; mobile phase, hexane.

Consequently, resistance to mass transfer in the bonded phases is not significantly greater for the bonded phases than for the unreacted silica. This conclusion is demonstrated further by the data in Table I. The *h* values are essentially independent of the k' values and the $n_{eff.}$/sec values are similar to the values measured for the μPorasil columns. It is also noteworthy that the μBondapak columns are operated at room temperature. In the case of the pellicular bonded polymer layers, columns most often have to be operated at elevated temperatures[27].

The poorer performance of the μBondapak CN column may be caused by a less ideal packing structure. The larger value of the intercept, the *A* term, of the *h vs. u* curve is an indication of a poorer packing structure.

In addition to column efficiency, another important characteristic of bonded phases is their selectivity. The μBondapak C_{18} column having a hydrophobic surface is useful as a high-efficiency reversed-phase packing. This packing is similar in selectivity to the pellicular bonded layer, Bondapak C_{18}/Corasil, and the totally porous material with $d_p = 37$–$75\,\mu$, Bondapak C_{18}/Porasil B. Table IV shows the relative retention data of a series of steroids run on all three columns. The reproducibility of the relative retention data is an indication of the ability to reproduce the chemical

TABLE IV

STEROID RELATIVE RETENTIONS IN THE BONDAPAK C_{18} SERIES

Mobile phase: acetonitrile–water (60:40); temperature: ambient.

Compound	*Packing*		
	Corasil	*Porasil*	*μPorasil*
Nortestosterone	1.0	0.9	0.9
Testosterone	1.0	1.0	1.0
Nortestosterone acetate	2.7	2.5	2.7
Testosterone benzoate	10.6	11.4	10.0
Testosterone propionate	23.0	24.5	25.2

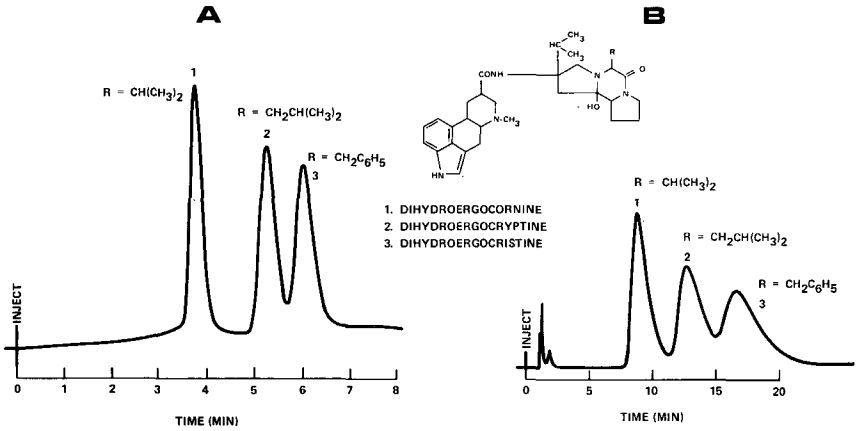

Fig. 6. Separation of some hydrogenated ergot alkaloids by reversed-phase chromatography. Column A: μBondapak C_{18}, 300 mm × 4 mm I.D.; mobile phase: acetonitrile–water (0.01 M $(NH_4)_2CO_3$) (40:60), 6 ml/min. Column B: Bondapak C_{18}/Corasil, 600 mm × 2 mm I.D.; mobile phase, acetonitrile–water (0.01 M $(NH_4)_2CO_3$) (33:67), 1 ml/min.

character of the bonded monomolecular layer. The use of small porous particles rather than pellicular materials gives the advantages of higher sample capacity and higher efficiency. A comparison of the separation of a series of structurally closely related compounds, hydrogenated ergot alkaloids, on the porous layer and the small-particle packing is shown in Fig. 6. Using the small-particle column the analysis can be done with better resolution with half the column length and in a much shorter time. Another example of the usefulness of the small-particle reversed-phase packing is the separation of the PTH derivatives of the amino acids using a gradient, Fig. 7. The components which are not separated by the gradient can be resolved using an isocratic mode. Fig. 8 shows the separation of a synthetic aromatic hydrocarbon mixture. Reversed-phase chromatography is more selective than LSC for the separation of aromatic hydrocarbons (compare Fig. 1).

Since the μBondapak CN has a hydrophobic surface it can also be used as a reversed-phase packing. Retention volumes are about five times smaller than those observed on the C_{18} columns. Fig. 9 shows the separation of some of the aromatics under the same experimental conditions as given in Fig. 8. The higher surface polarity of the CN packing is a probable explanation for this behavior. Excessively long retention volumes with large percentages of organic component of the mobile phase, *e.g.* acetonitrile, THF, etc., have often been observed with the C_{18} packing. The CN packing can have definite advantages in such situations. In addition, gradients would be expected to cover a broader range of solvent polarities in separations of complex mixtures. Differences in selectivity between the CN and C_{18} packings have not been investigated as yet. However, with the growing applicability of reversed-phase chromatography for the separation of a wide variety of organic compounds, the development of reversed-phase packings with different selectivities may prove to be an important use of bonded-phase packings.

The μBondapak NH_2 packing, having a hydrophilic surface, cannot be used as a reversed-phase packing. Along with the CN packing, it was investigated in normal

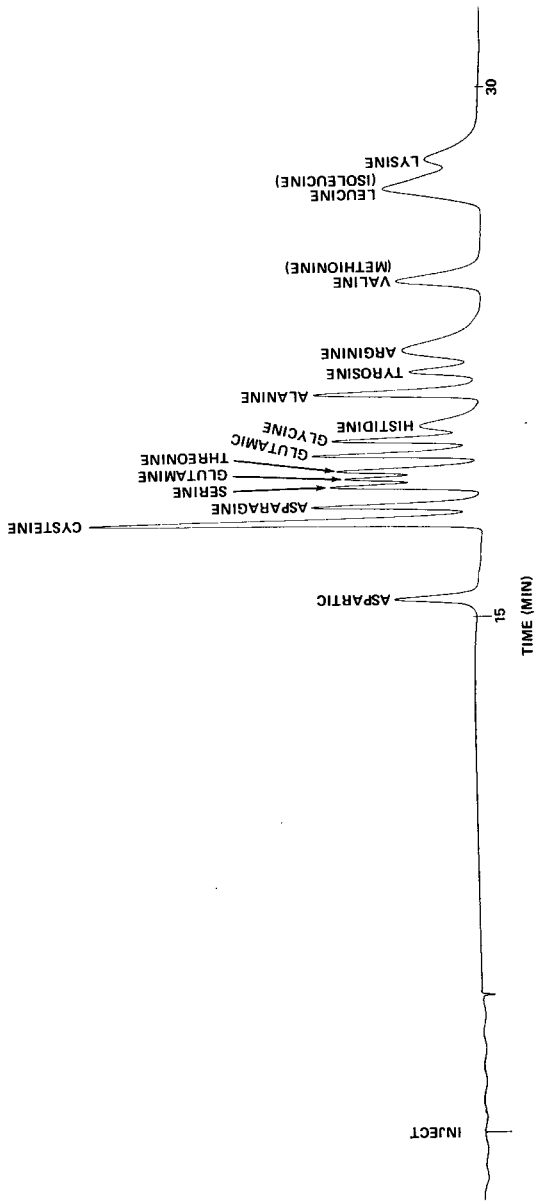

Fig. 7. Separation of phenylthiohydantoin (PTH) derivatives of amino acids on μBondapak C_{18} column. Column dimensions, 2 × 300 mm × 4 mm I.D. Gradient: solvent A, 0.01 *M* sodium acetate (pH 4); solvent B, acetonitrile; gradient profile concave, 5 to 50% acetonitrile; gradient time, 20 min; flow-rate, 2 ml/min.

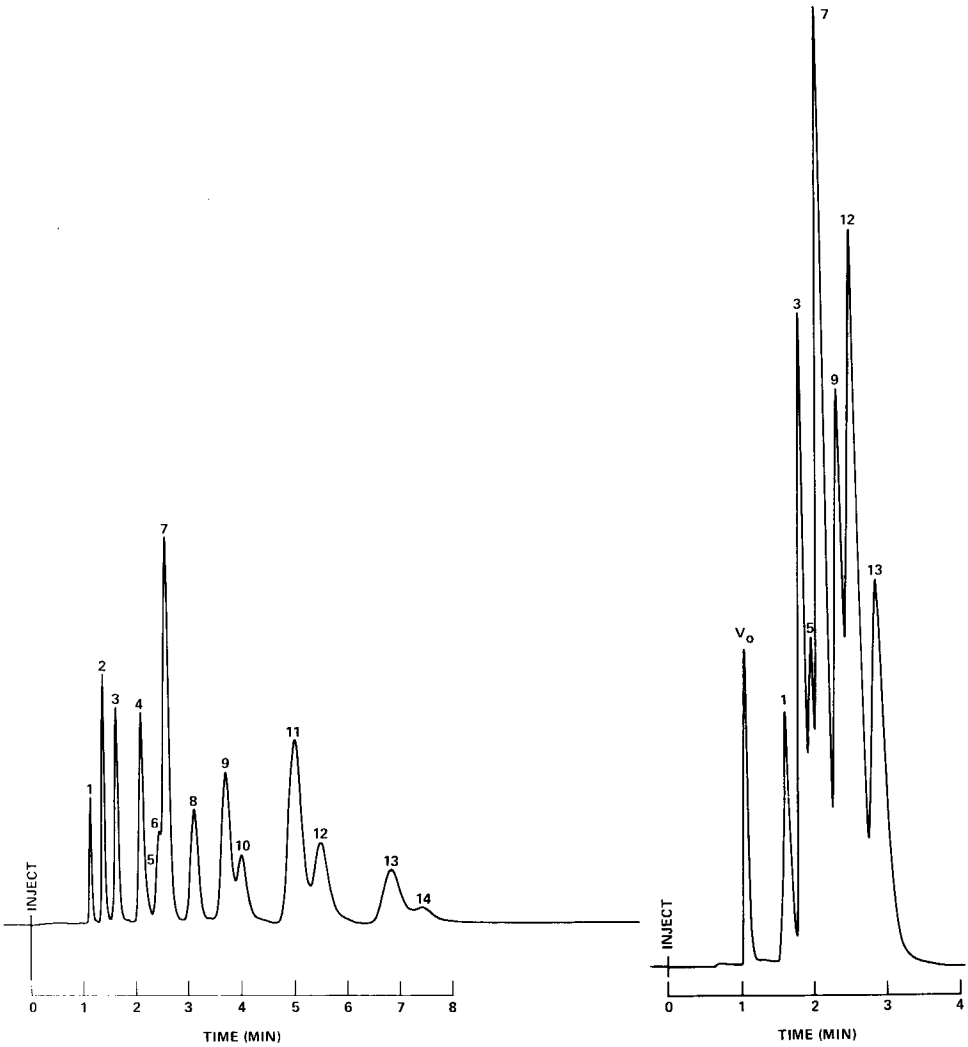

Fig. 8. Separation of a synthetic mixture of aromatic hydrocarbons on a μBondapak C_{18} column. Column dimensions, 300 mm × 4 mm I.D.; mobile phase, acetonitrile–water (60:40); flow-rate, 6 ml/min. Peak identifications: 1 = benzene; 2 = toluene; 3 = naphthalene; 4 = biphenyl; 5 = acenaphthene; 6 = phenanthrene; 7 = anthracene; 8 = pyrene; 9 = triphenylene; 10 = chrysene; 11 = 1,2-benzopyrene; 12 = 3,4-benzopyrene; 13 = 1,2,3,4-dibenzanthracene; 14 = 1,2,5,6-dibenzanthracene.

Fig. 9. Separation of polynuclear aromatics by reversed-phase chromatography on μBondapak CN column. Conditions, same as Fig. 8, except flow-rate 3 ml/min. Peak identifications, same as Fig. 8.

phase chromatography. The data in Table I show differences in selectivity towards the chloronitrobenzene isomers. A reversal in the elution order of the *meta* and *para* isomers is observed. The chromatogram is shown in Fig. 10. Note that the retentions are less on the CN packing, suggesting a lower surface polarity than the NH_2 packing. The NH_2 packing can also be used as an anion-exchange packing. The strongly basic

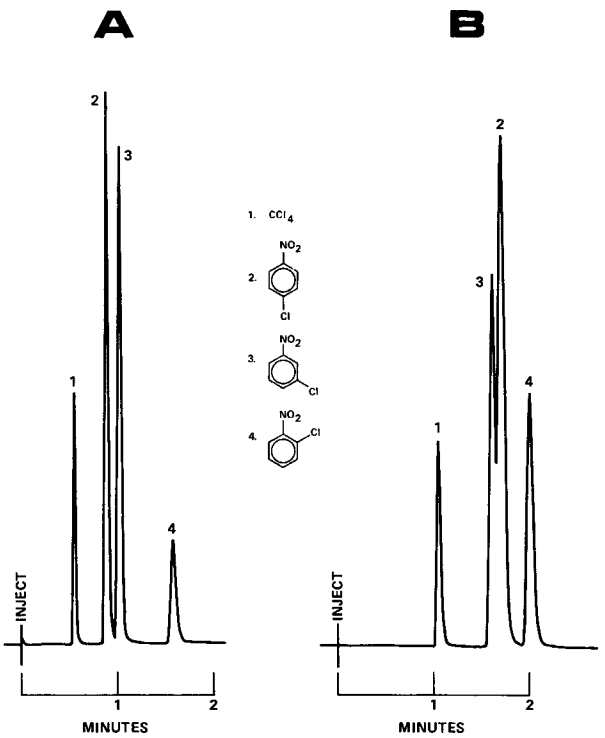

Fig. 10. Comparison of the separation of the chloronitrobenzene isomers on μBondapak NH_2 (A) and μBondapak CN (B) columns[13]. (A) Column, μBondapak NH_2, 300 mm × 4 mm I.D.; mobile phase, hexane, 6 ml/min; ΔP = 1500 p.s.i. (B) Column, μBondapak CN, 600 mm × 4 mm I.D.; mobile phase, hexane, 6 ml/min; ΔP = 3200 p.s.i.

NH_2 groups are protonated in acid solution to form the anion-exchange sites. Fig. 11 illustrates the use of the packing in this mode. The separation of the nucleoside 5'-phosphates on the pellicular strong anion exchanger, Bondapak AX/Corasil, took twice the amount of time and twelve times the column length.

Gel permeation chromatography

GPC is a basic technique encountered in the separation of polymeric materials on the basis of molecular size. In classical GPC, particle diameters of 37–75 μ, column lengths of 12 ft. or more, and low flow-rates (1 ml/min, 7 mm I.D. columns) are commonplace. Under such conditions, analysis times are excessively long —hours or longer. An increase in linear velocity to decrease analysis times can lead to a degradation in resolution. Since GPC is a diffusion-controlled separation process, the slow diffusion of polymers or large molecules in liquids explains the mobile phase velocity limitations of classical GPC. With large particles, $d_p > 30\,\mu$, diffusion distances are large within the packed bed and within the pores. Consequently, the linear velocity must be held low to allow sufficient diffusion time for achieving equilibrium.

A reduction in particle size promotes more rapid mass transfer; hence high mobile-phase velocities can be used. With small particles, solute diffusion distances are shorter within the packed bed, *e.g.* across particle diameter and within pore depths.

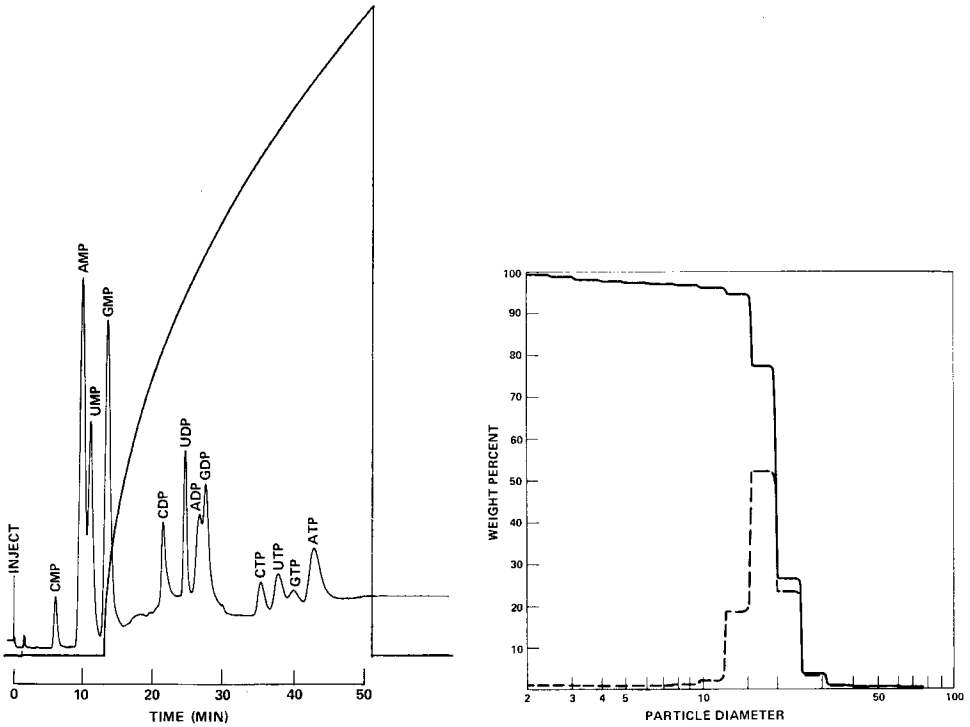

Fig. 11. Separation of the nucleoside 5′-phosphates on the μBondapak NH_2 column as an anion exchanger. Column dimensions, 300 mm × 4 mm I.D.; gradient, 0.01 *M* $NH_4H_2PO_4$ (pH 3.0) to 0.25 *M* $NH_4H_2PO_4$ (pH 5.0); gradient time, 45 min; flow-rate, 4 ml/min.

Fig. 12. Typical particle size distribution of a μStyragel sample.

Consequently, the solute molecules will undergo more rapid mass transfer between the mobile phase flow currents and in the stagnant mobile phase within the pores of the particle to produce faster and more efficient separations.

This work involves an investigation of the reduction in particle size of Styragel, a porous polymer available in a wide range of pore sizes, as a high-speed GPC packing. The standard Styragel product is available in a 37–75 μ fraction. Typical plate heights of packed Styragel columns are 0.3 mm or approximately 1000 plates/ft. using a totally permeating solute as toluene, at a linear velocity of 0.5 mm/sec.

To obtain high efficiency using small particles in GPC a narrow particle-size distribution is necessary[31]. The particle-size distribution shown in Fig. 12 is typical of materials used to obtain high-efficiency columns. Fig. 13 shows the *h vs. u* curves for packed columns of Styragel of varying particle size. The standard Styragel columns, d_p = 37–75 μ, show a rapid increase in *h* with increasing linear velocity. As the average particle size is reduced, plate heights are reduced as predicted by theory. The 18–25 μ, the 8–12 μ and the 3–8 μ fractions (curves B, C, D) show a much more gradual increase in *h* and a much higher efficiency over the range of linear velocity investigated. Interestingly, for both the 8–12 μ and the 3–8 μ fractions, minima in the *h vs. u* curves are observed. Such minima are not generally observed over the common

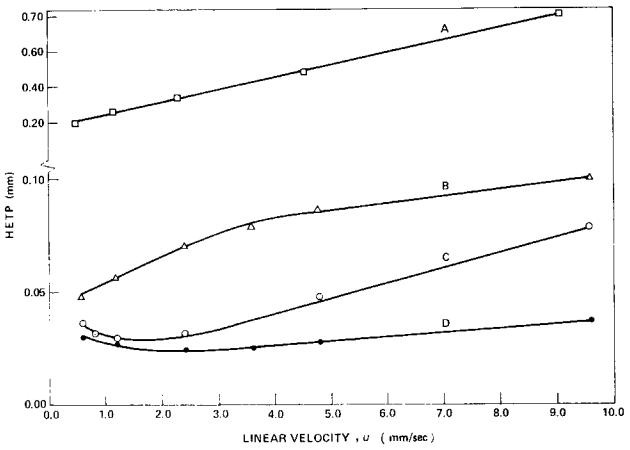

Fig. 13. Effect of particle size (d_p) of μStyragel on column efficiency. Solute, toluene; mobile phase, tetrahydrofuran; column dimensions, 2 × 300 mm × 7.6 mm I.D. (A) d_p = 37–75 μ; (B) d_p = 18–25 μ; (C) d_p = 8–12 μ; (D) d_p = 3–8 μ.

velocity ranges used in high-pressure LC. In GPC lower linear velocities are generally used. However, theory predicts that at very low linear velocities longitudinal molecular diffusion becomes an important contribution in the band spreading mechanism; consequently, an increase in h is noted in the low linear velocity region[32,33]. Working in this range is impractical in terms of resolution or fast analysis times. Note that for the 3–8 μ fraction the minimum is shifted to higher linear velocity than for the 8–12 μ fraction. Consequently, the advantages of a 3–8 μ fraction over the 8–12 μ fraction are minimal since much higher pressure drops for operation are necessary. Recently,

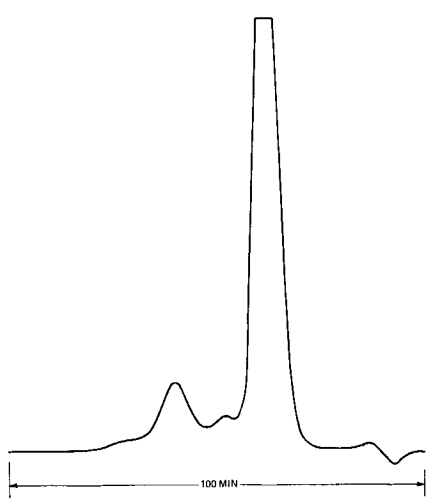

Fig. 14. Classical GPC separation of a liquid epoxy. Column dimensions, 5 × 120 cm × 7.6 mm I.D.; columns, Poragel of 10^3, 500, 250, 100, and 60 Å, d_p = 37–75 μ; mobile phase, tetrahydrofuran; flow-rate, 2 ml/min.

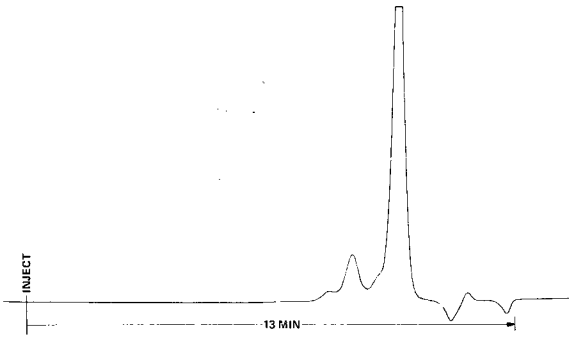

Fig. 15. High-speed GPC separation of a liquid epoxy. Column dimensions, 5 × 30 cm × 7.6 mm I.D.; columns, μStyragel of 500, 500, 500, 250, and 250 Å, d_p = 8–12 μ; mobile phase, tetrahydrofuran; flow-rate, 4 ml/min.

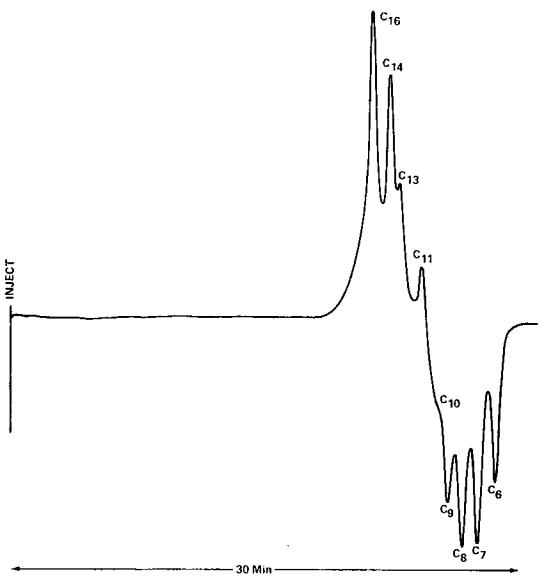

Fig. 16. GPC separation of normal hydrocarbons on μStyragel columns. Column dimensions, 4 × 300 mm × 7.6 mm I.D.; packing, μStyragel, 100 Å; mobile phase, tetrahydrofuran; flow-rate, 1 ml/min.

the disadvantages of 5-μ particles in high-speed GPC have been discussed[31]. The remainder of this paper deals with the practical utility of 10-μ Styragel® packed columns.

The practical utilities of high-speed GPC over classical GPC are many. The increased speed of analysis can be seen by comparing the separation of a liquid epoxy by classical GPC (Fig. 14) to the high-speed GPC using μStyragel (Fig. 15). To obtain the same resolution, the classical technique required 600 cm of column and an analysis time of 100 min. However, the same liquid epoxy was separated with 150 cm of μStyragel columns in 13 min, nearly an order of magnitude decrease in the analysis time.

To obtain higher resolution, the μStyragel columns can be run at slower linear velocities. In the high-resolution mode, even small molecules are readily separated. In Fig. 16 a separation of normal hydrocarbons using 120 cm of 100-Å μStyragel columns is shown. Similarly Fig. 17 shows the separation of a synthetic mixture of fatty acids.

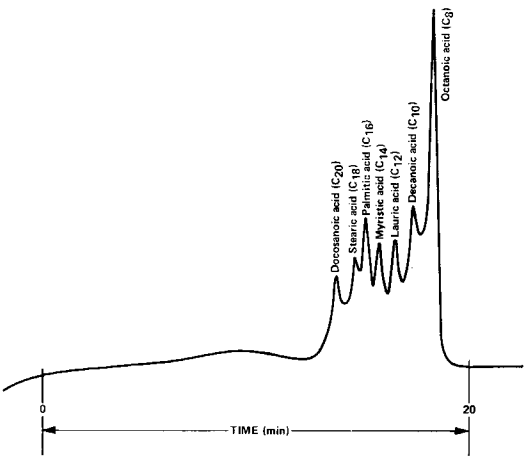

Fig. 17. High-resolution GPC separation of fatty acids. Conditions, same as Fig. 16.

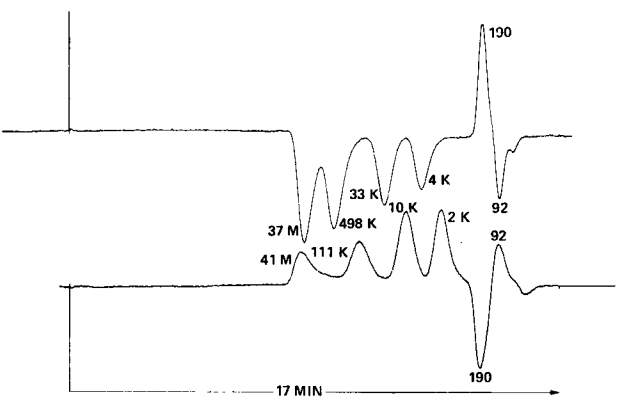

Fig. 18. High-speed GPC separation of polystyrene standards. Column dimensions, 5 × 30 cm × 7.6 mm I.D.; packing, μStyragel of 10^6, 10^5, 10^4, 10^3, and 500 Å; mobile phase, tetrahydrofuran; flow-rate, 4 ml/min.

The ease of obtaining a calibration curve is another advantage of high-speed GPC. Fig. 18 shows two chromatograms of polystyrene standards. The time needed for each separation was less than 17 min. Fig. 19 shows the calibration curve obtained by plotting the molecular weight peak *vs.* its elution volume. The entire calibration curve can be obtained in less than 1 h and checked periodically. These rapid analyses permit system stability checks without interfering with normal instrument use.

GPC is the simplest form of column chromatography. The separation mechanism is simply based upon molecular size. Other forms of chromatography —parti-

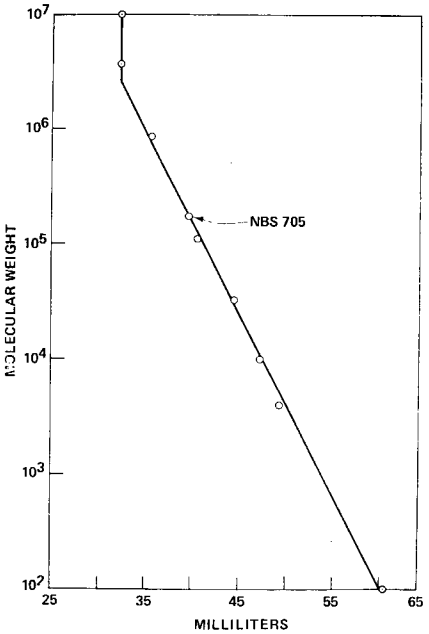

Fig. 19. Calibration curve of polystyrene standards from Fig. 18.

tion, adsorption, ion-exchange— have complex mechanisms which are not as well understood. The only information necessary to perform GPC separations is sample solubility and the sample's approximate molecular-weight distribution. High-speed GPC offers the chromatographer a simple and quick technique to characterize complex samples from small to large molecules based upon size, a rapid preparative technique and a useful method to clean up complex samples.

REFERENCES

1 R. E. Majors, *J. Chromatogr. Sci.*, 11 (1973) 88.
2 J. J. Kirkland, *J. Chromatogr. Sci.*, 10 (1972) 593.
3 R. E. Majors, *Anal. Chem.*, 44 (1972) 1722.
4 J. Asshauer and I. Halász, *J. Chromatogr. Sci.*, 12 (1974) 139.
5 J. J. Kirkland, *J. Chromatogr.*, 83 (1973) 149.
6 R. M. Cassidy, D. S. LeGay and R. W. Frei, *Anal. Chem.*, 46 (1974) 340.
7 J. F. K. Huber, *J. Chromatogr. Sci.*, 7 (1969) 85.
8 R. S. Deelder, P. J. H. Hendricks and M. G. F. Kroll, *J. Chromatogr.*, 57 (1971) 67.
9 J. F. K. Huber, *Chimia, Suppl.*, (1970) 24.
10 *Waters Ass. Data Sheet*, DS035, January, 1974.
11 I. Halász and I. Sebestian, *Angew. Chem., Int. Ed. Engl.*, 8 (1969) 453.
12 J. N. Little, W. A. Dark, P. W. Farlinger and K. J. Bombaugh, *J. Chromatogr. Sci.*, 8 (1970) 647.
13 I. Halász and I. Sebestian, *J. Chromatogr. Sci.*, 12 (1974) 161.
14 V. Bazant, V. Chvalousky and J. Rathousky, *Organosilicon Compounds*, Academic Press, New York, 1965, p. 212.
15 M. Novotný, S. L. Bektesh, K. B. Denson, K. Grohmann and W. Parr, *Anal. Chem.*, 45 (1973) 971.
16 M. Novotný, S. L. Bektesh and K. Grohmann, *J. Chromatogr.*, 83 (1973) 25.
17 J. J. Kirkland, *J. Chromatogr. Sci.*, 9 (1971) 206.

18 J. J. Kirkland and J. J. DeStefano, *J. Chromatogr. Sci.*, 8 (1970) 309.
19 W. A. Aue and C. R. Hastings, *J. Chromatogr.*, 42 (1969) 319.
20 C. R. Hastings, W. A. Aue and J. M. Augl, *J. Chromatogr.*, 53 (1970) 487.
21 C. R. Hastings, W. A. Aue and F. N. Larsen, *J. Chromatogr.*, 60 (1971) 329.
22 A. H. Al-Taiar, J. R. Lindsay Smith and D. J. Waddington, *Anal. Chem.*, 42 (1970) 935.
23 R. E. Majors, *Anal. Chem.*, 45 (1973) 755.
24 D. C. Locke, J. T. Schmermund and B. Banner, *Anal. Chem.*, 44 (1972) 90.
25 J. Wartmann and H. Duel, *Helv. Chim. Acta.*, (1959) 1166.
26 O.-E. Brust, I. Sebestian and I. Halász, *J. Chromatogr.*, 83 (1973) 15.
27 J. H. Knox and G. Vasvari, *J. Chromatogr.*, 83 (1973) 181.
28 K. Unger, *Angew. Chem., Int. Ed. Engl.*, 11 (1972) 267.
29 B. Evans and T. E. White, *J. Catal.*, 15 (1969) 307.
30 R. K. Iler, *The Colloid Chemistry of Silica and Silicates*, Cornell University Press, Ithaca, N.Y., 1955.
31 R. J. Limpert, R. L. Cotter and W. A. Dark, *Amer. Lab.*, May (1974) 64.
32 J. F. K. Huber and J. A. R. J. Hulsman, *Anal. Chim. Acta*, 38 (1963) 305.
33 J. F. K. Huber, *J. Chromatogr. Sci.*, 7 (1969) 85.